Trapped Modes In Waveguides with Many Small Discontinuities

Sergey Kurennoy
University of Maryland, Physics Department,
College Park, MD 20742, USA

Abstract

It has been demonstrated recently [1] that a single small discontinuity (such as an enlargement or a hole) on a smooth waveguide can result in the appearance of trapped electromagnetic modes with frequencies slightly below the waveguide cutoff frequencies. The present paper studies similar phenomenon for a waveguide with many small discontinuities, which is a good model for the vacuum chamber of large accelerators. Frequencies of trapped modes and their contributions to the coupling impedance are calculated. The frequencies for the cases of a few discontinuities or a periodic structure coincide well with those from numerical simulations. The trapped modes produce sharp resonance peaks of the coupling impedance near the cutoff frequencies. The magnitude of these peaks, as well as the existence itself of a trapped mode, strongly depends on the distribution of discontinuities, or on the distance between them if a regular array is considered. The impedance in the extreme case can be as large as N^3 times that for a single discontinuity, where N is the number of discontinuities.

1 Introduction

Previous computer studies of cavities coupled to a beam pipe indicated that the impedance of small chamber enlargements exhibits sharp narrow peaks at frequencies close to the cutoff frequencies of the waveguide, see references in [1]-[4]. For the case of a single small discontinuity, such as an enlargement or a hole, on a smooth waveguide it was demonstrated [1] that these peaks can be attributed to trapped modes localized near the discontinuity. The existence of a trapped mode depends on a relation between the conductivity of the chamber walls and a typical size of the discontinuity, and in the limit of perfectly conducting walls the trapped modes exist even for very small perturbations.

This phenomenon can be dangerous for the beam stability in large superconducting proton colliders like Large Hadron Collider (LHC), where the design anticipates a thermal screen (liner) inside the beam pipe [5]. The function of the liner is to screen the cold walls of the vacuum chamber from synchrotron radiation in order to prevent wall heating and photodesorption of

3 Many Discontinuities

Consider an axisymmetric waveguide with N small enlargements located at $z_1, z_2, \ldots z_N$ and having areas $A_1, A_2, \ldots A_N$ of the longitudinal cross section, respectively. In this structure, we will look for a solution of the Maxwell equations with frequency Ω slightly below the cutoff frequency ω_1. Let us introduce the propagation constant $k = \sqrt{\omega_1^2 - \Omega^2}/c$ and consider the following piece-wise form of the solution (only z-dependence is shown below, the radial behavior corresponds to Eq. (1) for $\mathcal{E}_z$, $\mathcal{E}_z$ and $\mathcal{H}_\theta$, respectively):

$$\begin{array}{rl} a_1 \exp(kz) \ , & \text{for} \quad z < z_1 \ , \\ a_{n+1} \exp(kz) + b_n \exp(-kz) \ , & \text{for} \quad z_n < z < z_{n+1} \ , \ n = 1, 2, \ldots, N-1 \ , \\ b_N \exp(-kz) \ , & \text{for} \quad z > z_N \ , \end{array} \tag{10}$$

where a_i, b_i, $n = 1, 2, \ldots, N$, are amplitudes to be determined. We assume, as well as in the case of a single discontinuity, that $kb \ll 1$, and the form of the solution above is justified when enlargements are spaced at least by the distance of the order of the chamber diameter, so that one can neglect higher modes which are essential only very close to discontinuities, namely, at distances a few times smaller than the chamber radius.

To find the eigenfrequency of the trapped mode we use continuity conditions and the Lorentz reciprocity theorem. It states that for any two solutions of Maxwell's equations without sources the following equality holds [6]

$$\int dS \vec{n} (\vec{E}_1 \times \vec{H}_2 - \vec{E}_2 \times \vec{H}_1) = 0 \ , \tag{11}$$

where the integration runs over a closed surface S consisting of the surface of the waveguide wall and two plane end surfaces which are transverse to the waveguide axis. We take $\vec{E}_1 = \vec{\mathcal{E}}$, $\vec{H}_1 = \vec{\mathcal{H}}$ and choose $\vec{E}_2, \vec{H}_2$ to be a TM mode having frequency Ω, the same as the trapped mode, and exponentially decaying either as $\exp(-kz)$ in the positive direction or as $\exp(kz)$ in the negative one. Due to the orthogonality of the radial eigenfunctions the only contribution to the end-surface integrals comes from terms with factor $\exp(kz)$ (or $\exp(-kz)$) opposite to that of the chosen TM mode. The only contribution to the wall integral comes from the regions of the waveguide enlargements, see [1] for more detail. We choose the positions of the end surfaces in such a way that the wall integration in Eq. (11) includes only one discontinuity at a time, and apply this procedure twice to all discontinuities in turn using first the TM mode with $\exp(-kz)$ behavior, and then with $\exp(kz)$. In fact, for the first and the last enlargements which belong to the semi-infinite intervals we use the integration with only one of the two possible TM modes. One more equation for each of these two discontinuities follows from the field continuity:

$$\begin{aligned} a_1 \exp(kz_1) &= b_1 \exp(-kz_1) + a_2 \exp(kz_1) \ , \\ b_{N-1} \exp(-kz_N) + a_N \exp(kz_N) &= b_N \exp(-kz_N) \ . \end{aligned} \tag{12}$$

Other $2N-2$ equations follow from the reciprocity as described above:

$$-a_1 + y_1 a_1 + a_2 = 0 \ ,$$

$$
\begin{aligned}
-a_n + y_n\left(a_n + b_{n-1}\exp(-2kz_n)\right) + a_{n+1} &= 0\,, \qquad & n = 2,\ldots,N-1,\\
-b_n + y_n\left(b_n + a_{n+1}\exp(2kz_n)\right) + b_{n-1} &= 0\,, \qquad & n = 2,\ldots,N-1,\\
-b_N + y_N b_N + b_{N-1} &= 0\,,
\end{aligned}
\tag{13}
$$

where the following notations are introduced: $y_n = d_n/x$, $d_n = \mu_1^2 A_n/b^2$ and $x = kb$. Combining (13) and (12) we get $2N$ simultaneous homogeneous equations for $2N+1$ variables: amplitudes a_i, b_i and propagation constant k. The condition for the solutions for a_i, b_i to exist, i.e. the determinant of the matrix in the left hand side of the equations above to vanish, gives us an equation for the propagation constant and, hence, for the frequency of the trapped mode.

Due to the structure of the matrix, which has three or less non-zero elements in each column or row, this equation can be written recurrently for any given number N in terms of all the LHS of the equations for lower numbers of discontinuities. In the notations introduced above, Eq. (2) for $N = 1$ can be rewritten as

$$1 - y = 0\,,$$

where $y = d/x$ with $d = \mu_1^2 A/b^2$ and $x = kb$. The small parameter d is just the ratio of the waveguide radius b to the length l_1 of the region occupied by the fields of the trapped mode for a single discontinuity, cf. Eq. (2). For the case $N = 2$ from (13) and (12) we get

$$D_{1,2}(k) \equiv (1-y_1)(1-y_2) - \exp(-2kg_{1,2})y_1y_2 = 0\,, \tag{14}$$

where $g_{i,k} = z_k - z_i$, $(k > i)$, is a longitudinal spacing between i-th and k-th discontinuities. Similarly, for $N = 3$ the equation is

$$D_{1,3}(k) \equiv D_{1,2}(k)D_{2,3}(k) - \exp(-2kg_{1,3})y_1y_3 = 0\,. \tag{15}$$

For the case of $N > 3$ discontinuities the equation can be written in the following form:

$$D_{1,N}(k) \equiv D_{1,N-1}(k)D_{N-1,N}(k) - \sum_{m=2}^{N-2} D_{1,m}(k)\exp(-2kg_{m,N})y_m y_N - \exp(-2kg_{1,N})y_1y_N = 0\,, \tag{16}$$

that can be proved by induction. Multiplying by k^{2N-2} the LHS of the equation one can reduce it to a polynomial of the power $(2N-2)$ in k except the exponential dependence on k in its coefficients.

3.1 N=2

To study the frequencies of trapped modes in the system of two discontinuities, it is convenient to introduce new variables:

the ratio of areas of two enlargements $\rho = A_2/A_1 > 1$;

$d = \mu_1^2 A_1/b^2$;

variable $u = x/d$ is the ratio of the propagation constant k for a $N = 2$ trapped mode to that in the case of a single discontinuity, k_1, given by Eq. (2) with $A = A_1$, and

parameter $r = gd/b = g/l_1$ is the ratio of the distance between discontinuities to the length l_1 of the region occupied by the trapped mode for a single discontinuity with area A_1, i.e. $l_1 = b/d = b^3/(\mu_1^2 A_1)$, cf. Eq. (2).

In these notations, Eq. (14) takes the form

$$(u-1)(u-\rho) - \rho\exp(-2ur) = 0 \ . \tag{17}$$

We are interested only in positive solutions of this equation. Factorizing it as product of two "linear" equations

$$\begin{aligned} &\left(2u - \rho - 1 - \sqrt{(\rho-1)^2 + 4\rho\exp(-2ur)}\right) \ \times \\ &\left(2u - \rho - 1 + \sqrt{(\rho-1)^2 + 4\rho\exp(-2ur)}\right) \ = \ 0 \ , \end{aligned} \tag{18}$$

one can easily find out that there are two positive solutions. The first one, u_s, exists for any positive value of parameter r and decreases asymptotically in the range from $\rho + 1$ at small r to ρ when $r \gg 1/\rho$. The second solution, u_a, exists only for $r > (\rho+1)/(2\rho)$, and increases asymptotically from 0 to 1 with r increase (see Fig. 1 for $\rho = 2$). The asymptotic values ρ and 1 obviously correspond to the two independent trapped modes for the two discontinuities separated so far that they do not feel each other, and each mode is described separately by Eq. (2).

The case of two identical discontinuities, $\rho = 1$, is very intersting. The factorized Eq. (18) is especially simple in this case:

$$[u - 1 - \exp(-ur)]\,[u - 1 + \exp(-ur)] = 0 \ , \tag{19}$$

and both its solution tends to 1 at large r. The physical interpretation of the two possible solution can be easily found from Eqs. (12)-(13): u_s gives a symmetric field and u_a an antisymmetric one, i.e. the fields are zero in the midpoint between the two identical enlargements for the second solution. The antisymmetric solution exists only for large spacings, see Fig. 2, and its frequency shift is always smaller than that for a single discontinuity with the same area. It should be noted here that frequency shifts are assumed to be small compared to the cutoff frequency, and they are approximately proportional to u^2, cf. Eq. (3).

The behavior of the symmetric solution u_s at small r is also easy to explain: when two enlargements are very close to each other they work like a single enlargement with area $A = A_1 + A_2$. It corresponds to the limit $u_s \to \rho + 1$ in the general case of two discontinuities (and $u_s \to 2$ for two identical ones) when $r \to 0$.

It is appropriate to mention an obvious analogy of the problem under consideration with the well-known problem of two narrow potential wells in quantum mechanics.

To check our analytical results for frequencies, we have carried out numerical computations of the lowest eigenfrequencies in a long cylindrical resonator with two small pill-boxes by means of the code SUPERFISH [7] varying the distance between the pillboxes. The waveguide cut-off frequency ω_1 corresponds to the eigenfrequency of E_{010}-mode in the smooth (without pill-boxes)

resonator with the same radius, but the presence of enlargements shifts the eigenfrequency down. To exclude the influence of the side walls, one has to choose length L of the resonator to be larger than the region where the trapped mode is localized, $L \gg l_1 = b^3/(\mu_1^2 A)$. We have used $b = 2$ cm, $A_1 = A_2 = A = 0.18$ cm^2, g =1–20 cm and L from 40 cm to 100 cm. Fig. 2 shows that numerical and analytical results are in good agreement. Fig. 3 and 4 show the electric field lines for resonator eigenmodes that correspond to the symmetric and antisymmetric trapped modes in the waveguide with two enlargements (only one quarter of the longitudinal cross section of the resonator is shown).

The resonant contributions of trapped modes to the beam-chamber coupling impedance can be calculated in the same way as in the case of a cavity with known eigenmodes, see Reference [4] for details. The peak value of the longitudinal impedance in the resonance can be evaluated as

$$R_2 = \frac{\sigma\delta\,|\int dz \exp(-i\Omega z/c)\mathcal{E}_z(z)|^2}{\int_S ds|\mathcal{H}_\tau|^2}\,, \tag{20}$$

where $\mathcal{H}_\tau$ is the tangential component of the magnetic field near the wall, integration in denominator is performed over the inner waveguide surface, σ is conductivity of the pipe wall, and $\delta = \sqrt{2/(\mu_0\sigma\omega_1)}$ is the skin depth. Performing the integration and taking into account that the frequency Ω of the trapped mode is very close to the cutoff frequency $\omega_1 = \mu_1 c/b$ lead to the expression

$$R_2 = R_1 u^3 \frac{u(1+\rho) + 2\rho\,[\exp(-ur)\cos(\mu_1 g/b) - 1]}{u(1+\rho) + 2\rho\,[\exp(-2ur)(1+ur) - 1]}\,, \tag{21}$$

where $R_1 = (4Z_0\mu_1 A_1^3)/(\pi\delta b^5 J_1^2(\mu_1))$ is just the impedance for a single enlargement with area A_1, cf. Eq. (6), and $u = u(r,\rho)$ is a solution of Eq. (17).

The extreme cases of small ($r \to 0$) or large ($r \gg 1$) distances between discontinuities can be derived easily basing on the study of Eq. (17) above. For small r the ratio of impedances of two discontinuities to the impedance of the smallest one of them, R_2/R_1, tends to $(1+\rho)^3$ for the "symmetric" solution u_s. For large distances, R_2/R_1 becomes ρ^3 for u_s and 1 for u_a. There are some oscillations at intermediate distances, see Fig. 5.

Expression (21) takes even more simple form for the case of two identical discontinuities, $\rho = 1$:

$$R_2 = R_1 \frac{u^3\,(1 \pm \cos(\mu_1 g/b))}{1 \pm \exp(-ur)(1+ur)}\,, \tag{22}$$

where the upper sign corresponds to the symmetric solution $u = u_s(r)$ which satisfies $u - 1 - \exp(-ur) = 0$, and the lower one to the antisymmetric solution $u = u_a(r)$ which satisfies $u - 1 + \exp(-ur) = 0$. The asymptotic behavior of (22) at large distances can be found using asymptotics $u_s \to 1 + e^{-r}$ and $u_a \to 1 - e^{-r}$. The ratio R_2/R_1 becomes $(1 \pm \cos(\mu_1 g/b))$. While the sum of these impedances is just twice the impedance of a single enlargement, there are strong oscillations for each of two modes.

The ratio R_2/R_1 is plotted in Fig. 5 for $\rho = 2$ and in Fig. 6 for $\rho = 1$.

3.2 N=3

We restrict ourselves here only to the case of three identical equidistant discontinuities, i.e. $d_i = d$, $i = 1,2,3$ and $g_{1,2} = g_{2,3} = g$. The equation (15) transforms into the following factorized equation:

$$(u-1)(u-1+\exp(-2ur))\left[(u-1)^2-(u+1)\exp(-2ur)\right] = 0 \ , \tag{23}$$

where again $u = kb/d = k/k_1$ and $r = gd/b = g/l_1$. One can easily recognize that the expression in the second brackets gives an antisymmetric trapped mode for two enlargements spaced by $2g$, compare Eq. (19), and the enlargement in the middle just does not play in this case since the trapped mode fields vanish near its location. The first brackets gives an extraneous root, while the "quadratic" equation in the square brackets has two positive solutions which correspond to symmetric trapped modes. The first solution, u_{s0}, corresponding to fields without nodes, exists for all positive values of r and tends to 3 at small r. The second one, u_{s1}, exists only when $r > 3/2$ and gives a trapped mode with 2 nodes. All three solution goes asymptotically to 1 at large distances between discontinuities. Fig. 7 shows the three solutions of Eq. (23) versus the spacing between discontinuities, as well as comparison with results of some numerical computations using SUPERFISH.

The impedance for the antisymmetric trapped mode is given by Eq. (22) with the minus sign where $g \to 2g$ and $r \to 2r$ should be substituted. For the symmetric modes one can obtain

$$R_3 = R_1 u \frac{(\exp(ur)(u-1)+\exp(-ur)+2u\cos(\mu_1 g/b))^2}{3u+1-\exp(-2ur)+4ur(u-1)} \ . \tag{24}$$

The derivation and notations used are similar to those of Eq. (21). At small distances, ratio R_3/R_1 for the maximal symmetric mode u_{s0} goes to $3^3 = 27$, and at large distances oscillates as $(1+\sqrt{2}\cos(\mu_1 g/b))^2/2$. The second symmetric mode exhibits similar oscillations $(1-\sqrt{2}\cos(\mu_1 g/b))^2/2$ at large r. The impedance versus the distance between discontinuities is plotted in Fig. 8. In spite of the oscillations for each of the trapped modes, the sum of the impedances for all three modes becomes just triple of that for a single discontinuity at large spacings in which case all three modes have the same frequency, given by Eq. (3).

3.3 Many Identical Discontinuities

In the case of N identical equidistant enlargements one should put $y_i = y$, $i = 1,2,\ldots,N$ and $g_{i,i+1} = g$, $i = 1,2,\ldots,N-1$ in equation (16). The resulting equation has the following properties.

It can be factorized in the form

$$(1-y)^{N-2}P_n(y)P_m(y) = 0 \ , \tag{25}$$

where n, m are integers satisfying $n+m = N$ so that

$$n = \begin{cases} m & \text{for } N = 2m \\ m+1 & \text{for } N = 2m+1 \end{cases}$$

and $P_n(y), P_m(y)$ are polynomials in y of the power n and m except exponential dependence on $u = 1/y$ in their coefficients, cf. Eqs. (19) and (23) above. Equation $P_n(y) = 0$ has up to n positive solutions corresponding to symmetric trapped modes. The actual number of the roots depends on the distance g between discontinuities. It can be proved by induction that for any g there is at least one solution, and it behaves like $y \simeq 1/N$ at small distances, i.e. $k \simeq Nk_1$, because $P_n(y) \to 1 - Ny$ when $g/l_1 \to 0$. This solution corresponds to the maximal symmetric trapped mode, without nodes, as was discussed in two subsections above for $N = 2$ and $N = 3$. It always has the largest frequency shift, i.e. the lowest frequency between all the trapped modes.

Equation $P_m(y) = 0$ gives up to m solutions corresponding to antisymmetric trapped modes. At large distances, when $g/l_1 \gg 1$, the asymptotics of $P_j(y)$, $j = n, m$, are $(1-y)^j$, and there are $N = n + m$ solutions of Eq. (25) which asymptotically tend to 1. The degenerated roots $y = 1$ due to the explicit factor in Eq. (25) are extraneous ones.

As follows from discussions in previous subsections, the physical interpretation of the both extremal cases, at small and large spacings, is quite obvious. At small distances between discontinuities they work together as a single combined discontinuity with effective area $A = A_1 + A_2 + \cdots + A_N$, that gives the maximal symmetric trapped mode with $k \simeq Nk_1$ for identical discontinuities. At large separations, the discontinuities do not feel each other, and there exist N independent trapped modes, each localized around one of the discontinuities. These modes can be described by the equations of Section 2 for a single discontinuity.

Pictures of subsections $N = 2$ and $N = 3$ give some impression about frequencies and impedances of trapped modes for these particular cases. In addition, Fig. 9 gives an illustration of the solutions to Eq. (25) in the case of $N = 6$. There are three symmetric and three antisymmetric trapped modes.

4 Many Discontinuities: Periodic Structures

4.1 One Discontinuity per Period

In this section periodic arrays of discontinuities are considered. We assume that the period of the structure D is longer than the waveguide diameter, $D > 2b$, and look for a periodic (with the same period D) solution of the Maxwell equations with frequency Ω below the waveguide cutoff, $\Omega < \omega_1$. As well as above, we restrict ourselves to TM-like solution with radial behavior given by Eq. (1), taking into account, however, that the same way of reasoning works for TE-modes. Let us consider one period $-D/2 < z < D/2$ with an enlargement located at $z = 0$. Similar to Eq. (10) and using the same notations, one can write z-dependence of the solution as

$$\begin{aligned} a\exp(kz) + b_{-1}\exp(-kz)\ , &\qquad \text{for} \quad -D/2 < z < 0\ , \\ b\exp(-kz) + a_1\exp(kz)\ , &\qquad \text{for} \quad 0 < z < D/2, \end{aligned} \tag{26}$$

where amplitudes a, b correspond to the waves originated from the enlargement at $z = 0$, the wave with amplitude b_{-1} comes from the previous period of the structure with the center at

$z = -D$, and the wave with amplitude a_1 comes from the next period, with the center at $z = D$. From periodicity follows that

$$b_{-1} = b\exp(-kD); \qquad a_1 = a\exp(-kD) \ . \tag{27}$$

To find the frequency of the trapped mode we use continuity conditions and the reciprocity. The continuity at $z = 0$ requires

$$a + b_{-1}\exp(-kD) = b + a_1\exp(kD) \ .$$

Taking into account relations (27), it gives

$$(a - b)(1 - \exp(-2kD)) = 0 \ .$$

Since we consider $k > 0$, this equation leads to $a = b$, while other solutions, $k = i\pi m/D$, correspond to space harmonics with frequencies above the cutoff.

Applying the reciprocity theorem for the trapped mode under consideration and a regular waveguide TM-mode with the same frequency Ω, we get a simple equation for propagation constant k:

$$y - 1 + \exp(-kD)(y + 1) = 0 \ , \tag{28}$$

where, as well as in previous sections, $y = d/(kb)$ with $d = \mu_1^2 A/b^2 \ll 1$. Using new variables $u = 1/y = k/k_1$ and $p = dD/b = D/l_1$, one can rewrite it as follows

$$u = \frac{1 + \exp(-up)}{1 - \exp(-up)} \ . \tag{29}$$

A simple study shows that this equation has only one positive solution $u = u(p) > 1$ for any positive value of p, see Fig. 10. Asymptotics for long periods, $u(p) \simeq 1 + 2\exp(-p)$ when $p \gg 1$, obviously corresponds to the trapped mode for a single discontinuity, cf. Section 2.

The opposite asymptotics, at $p \ll 1$, is quite different from the asymptotics in the case of a finite number of discontinuities, when it tends to a finite limit (Section 3). For periodic structures, the short-period behavior is

$$u(p) \simeq \sqrt{2/p} = \sqrt{2l_1/D} \quad \text{for} \quad p \ll 1 \ . \tag{30}$$

Since $u = l_1/l$ where $l_1 \equiv 1/k_1$ has the meaning of the length of the region occupied by the trapped mode for a single discontinuity, cf. Eq. (2), and $l \equiv 1/k$, it gives a new "effective" length of the trapped mode in a periodic structure

$$l \simeq \sqrt{\frac{Dl_1}{2}} = \frac{b}{\mu_1}\sqrt{\frac{Db}{2A}} \ . \tag{31}$$

The frequency shift down from the cutoff frequency for this trapped mode becomes

$$\Delta\omega = \omega_1 \frac{\mu_1^2}{2}\left(\frac{Au}{b^2}\right)^2 = \omega_1 \frac{A}{bD} \ . \tag{32}$$

This simple answer has also a simple physical explanation. For a closed cylindrical cavity resonator of length D and radius b with a small axisymmetric enlargement, having area A in the longitudinal cross section, on its side surface, the eigenfrequency of a given TM-mode ω_0 shifts down due to the enlargement presence, e.g. [8]:

$$\frac{\Delta\omega}{\omega_0} = \frac{1}{2}\frac{\int_{\Delta V} dV(|H|^2 - |E|^2)}{\int_V dV|H|^2} \propto \frac{A}{bD}, \tag{33}$$

where E, H are the fields in the resonator without enlargement, ΔV and V mean volumes of the enlargement and cavity. In the transition to the last expression in the RHS is taken into account that $|E| \ll |H|$ near the cavity wall. So, the relative frequency shift is proportional to the ratio of the volumes of the enlargement and cavity, as well as in Eq. (32).

One can imagine metallic transverse end planes in the middle between every two discontinuities in a periodic structure so that it transforms in a chain of adjacent identical cavities. Such walls do not change the fields and frequencies of trapped modes in the waveguide. However, the analogy between Eqs. (32) and (33) works only when the fields fill the whole cavity, from one end wall to the other. It is exactly the case of trapped modes in short-period structures when $D \ll l_1$. One the other hand, for long periods ($D \gg l_1$) the argument of a closed cavity fails since the fields in a trapped mode do not reach the end walls, and that is why the frequency shift is independent of the length of resonators.

It is appropriate to mention that starting from the well-known relation (33) one can easily derive qualitatively the frequency shift of the trapped mode for a single discontinuity, Eq. (2). Indeed, if the mode frequency is given by Eq. (33), its propagation constant is

$$k \simeq \sqrt{2\omega_0\Delta\omega}/c = \mu_1/b\sqrt{2A/(bD)}\ ,$$

and the length of the mode propagation

$$l = 1/k = b/\mu_1\sqrt{bD/(2A)}\ .$$

These relations work until $l > D/2$, otherwise fields tear off the end surfaces of the resonator. One can estimate the resonator length when it occurs by putting $D = 2l$ in the equation above. If D becomes larger, the mode frequency does not change any more because the fields do not reach the end walls. It gives

$$l = b^3/(\mu_1^2 A)\ ,$$

that is exactly the same as follows from Eq. (2). Of course, the coincidence of the numerical factors is just by accident.

It is clear from the discussion above that one can check Eq. (32) by numerical computations using SUPERFISH [7] even easier than in previous sections when one had to use very long resonators in order to avoid the influence of the end walls. The results of our numerical calculations for various resonator lengths (i.e., various periods) are shown in Fig. 10 and coincide well with the results from Eq. (32). Fig. 11 shows fields of trapped modes calculated by the code for two periodic structures.

The resonant coupling impedance per period produced by a trapped mode can be calculated in the same way as above, cf. Eq. (20), except the integration over z should be limited to one period. The result is a rather complicated expression

$$\begin{aligned} R_p &= R_1 \frac{u}{d^2\,(1-\exp(-up))} \left[\mu_1^2 e^{-up} \sin^2\left(\frac{\mu_1 D}{2b}\right) + 2\mu_1 u d e^{-up/2} \sin\left(\frac{\mu_1 D}{2b}\right) \right. \\ &\times \left. \left(1 - e^{-up/2}\cos\left(\frac{\mu_1 D}{2b}\right)\right) + u^2 d^2 \left(1 - e^{-up/2}\cos\left(\frac{\mu_1 D}{2b}\right)\right)^2 \right] , \end{aligned} \tag{34}$$

where $u = u(p)$ is a solution of Eq. (32), and R_1 is given by (6). The asymptotics of the impedance are:
for large distances ($p \gg 1$), $R_p \to R_1$, i.e. to the impedance of a single discontinuity;
for short distances ($p \ll 1$),

$$R_p \to \frac{R_1}{d^3}\frac{\mu_1^2 b}{D}\sin^2\left(\frac{\mu_1 D}{2b}\right) = \frac{Z_0}{\pi \mu_1^2 J_1^2(\mu_1)}\frac{2b}{\delta}\frac{\sin^2[\mu_1 D/(2b)]}{\mu_1 D/(2b)} .$$

An interesting feature of the last expression is that it is independent of enlargement area A, except that this asymptotic is valid when $2b < D \ll l_1 = b^3/(\mu_1^2 A)$, while in the opposite extreme $R_p \to R_1 \propto A^3$. Since A is considered to be small ($d = \mu_1^2 A/b^2 \ll 1$), the impedance per period is much larger for short-period structures. It is illustrated by Fig. 12, which shows the impedance per period versus the period length.

4.2 A Few Discontinuities per Period

Let us consider shortly the case when there are more than one enlargement per period of a periodic structure. Once again we introduce unknown amplitudes of a piece-wise solution, apply restrictions from continuity, periodicity and reciprocity to obtain a linear system of equations for the amplitudes. For the case of N enlargements, there are $2N+1$ variables ($2N$ amplitudes and one propagation constant k) and $2N$ homogeneous equations. In fact, they differ from Eqs. (12)-(13) only by two first and two last equations (for the first and last enlargement), due to periodicity. The requirement of the determinant of the matrix $M_{2N}(k)$ in the LHS of the linear system to vanish gives an equation to solve for k. We restrict ourselves only by the example of $N = 2$, in which case this equation takes the form:

$$\begin{aligned} \det M_2(k)/[(1-y_1)(1-y_2)] &= (1-y_1)(1-y_2) - e^{-2kg} y_1 y_2 - 2e^{-kD} \\ &+ e^{-2kD}(1+y_1)(1+y_2) - e^{-2k(D-g)} y_1 y_2 = 0 , \end{aligned} \tag{35}$$

where D is the structure period, g is the distance between the discontinuities, $g \le D$, and y_n are defined after Eq. (13). For long periods, $kD \gg 1$, Eq. (35) becomes just Eq. (14). For short distances g, when $kg \ll 1$, Eq. (35) gives the same as Eq. (28) for one enlargement per period, but with $y = y_1 + y_2$, i.e. we have a single combined discontinuity.

When two discontinuities are identical, $y_1 = y_2 = y$, Eq. (35) transforms into a product of two following equations ($u = 1/y$):

$$u = \frac{1 + \exp(-up) + \exp(-ur) + \exp(-u(p-r))}{1 - \exp(-up)}, \tag{36}$$

$$u = \frac{1 + \exp(-up) - \exp(-ur) - \exp(-u(p-r))}{1 - \exp(-up)}, \tag{37}$$

where $p = dD/b$ and $r = dg/b$, $r \leq p$. The first of this equations in the particular case $D = 2g$ transforms into Eq. (29) with p replaced by r, that corresponds to a structure with period g and one discontinuity per period. The second equation in the same particular case gives, for D large enough, one more solution, which can be recognized as corresponding to an antisymmetric trapped mode. We missed this mode earlier, studying the case of a single discontinuity per period, because the study was restricted to solutions having the same period as the structure. The antisymmetric mode in this case has twice longer period. In general case, this solution exists when (i) p is large enough, and (ii) both $\kappa = r/p = g/D$ and $(1 - \kappa)$ are not very small. It is illustrated by Fig. 13, where solution $u_a(p, r)$ of Eq. (37) is plotted as the function of p and κ. The same plot for solution $u_s(p, r)$ of Eq. (36) is shown in Fig. 14. One can see that the frequency shift for the antisymmetric mode is always smaller than that for a single discontinuity ($u = 1$), while for symmetric solutions it is always larger.

5 Effects of Trapped Modes in Liners

It should be reminded that the results above are applicable to vacuum chambers not only with small enlargements but also with small pumping holes. The only difference is that for holes one should replace area A of the enlargement cross section in all formulas by an "effective" area, as was mentioned in Section 2. Say, if there are M holes in one transverse cross section of a cylindrical vacuum chamber, for an axisymmetric trapped mode the following substitution takes place

$$A \rightarrow \frac{\alpha_{\theta 1} + \alpha_{\theta 2} + \cdots + \alpha_{\theta M}}{4\pi b}, \tag{38}$$

where α_{θ_m}, $m = 1, 2, \ldots, M$, denotes the magnetic susceptibility in the azimuthal direction of the mth hole in this transverse row, b is the chamber radius. The sum occurs because all small pumping holes, having the same longitudinal position, contribute to the trapped mode additively, working as a single discontinuity. Holes at another longitudinal location work as another combined discontinuity. As follows from the results above, one can consider two small holes as having the same longitudinal position if their separation along the chamber axis is shorter than the chamber radius.

Bearing this in mind, we shall study trapped modes in a liner of a superconducting accelerator and give estimates of their contribution to the coupling impedance. As an example, we refer to the LHC vacuum chamber. Its present design anticipates inside the chamber a stainless-steel thermal screen (liner) with the wall thickness $t \simeq 1$ mm, having a square transverse cross section

with rounded corners, 50 mm in diagonal, and a thin copper coating of the inner wall surface. To minimize the low-frequency coupling impedances, the pumping holes will have a shape of rounded-end narrow slots with length $s = 6$ mm and width $w = 1.5$ mm. The total pumping surface is 4% of the wall surface, this fraction was chosen from vacuum requirements. There are 666 pumping slots per meter of liner, with $M = 8$ slots in one transverse cross section, and the londitudinal separation between adjacent cross sections with the slots is $g = 1.2$ cm. Taking into account that TM-modes in a square, rounded-end waveguide are quite similar to those in a cylindrical one, we will take for estimates the "effective" chamber radius $b = 18$ mm. Then expression (38) takes the form

$$A \rightarrow \frac{M\alpha_\theta}{4\pi b} = \frac{Mw^2 s}{4\pi^2 b} , \tag{39}$$

where we use transverse magnetic susceptibility $\alpha_\theta = w^2 s/\pi$ for a narrow long slot in the thick wall, because $t \simeq w$, see, e.g. in [9, 10]. As the result, the "effective" area to be substituted in formulae of Sections 3 and 4 is $A = 1.52 \cdot 10^{-3}$ cm^2. The length of the region which would be occupied by the field of the trapped mode for a single such discontinuity is $l_1 = b^3/(\mu_1^2 A) =$ 6.63 m, cf. Eq. (2). Since this is much longer than the distance between adjacent discontinuities, they strongly interact each other, and because $g \ll l_1$, this situation is described by Eqs. (30)-(32) with $D = g = 1.2$ cm. It means that $u = \sqrt{2l_1/g} \simeq 33$, and the new "effective" length of interaction $l = \sqrt{l_1 g/2} = 20$ cm. If we define the number of discontinuities which work as a single combined discontinuity by $N_{eff} = 2l/g$, one can easily see that $N_{eff} = u = 33$. The frequency shift for the trapped mode is given by Eq. (32):

$$\frac{\Delta\omega}{\omega_1} = 7 \cdot 10^{-4} ,$$

that is $\Delta f \simeq 5$ MHz for $f_1 \simeq 6.4$ GHz. The gap between the trapped mode frequency and the cutoff is rather small, and one has to compare it with the width of the resonance due to energy dissipation in the walls and due to radiation from the slots: $\gamma = \gamma_1 + \gamma_{rad}$. According to Eq. (4),

$$\frac{\gamma_1}{\omega_1} = \frac{\delta}{2b} \simeq \frac{2.3 \cdot 10^{-5}}{\sqrt{RRR}} ,$$

where RRR is the ratio of the copper conductivities at cryogenic and room temperatures, which is usually 30–100. The radiation width for a thin wall would be [1]:

$$\frac{\gamma_{rad}}{\omega_1} \simeq N_{eff} M \frac{\mu_1^3 k \alpha_\theta^2}{3b^5} \simeq 6 \cdot 10^{-5} .$$

However, for the thick wall, the external magnetic susceptibility $\alpha_{ext} \simeq \exp[-\pi t/(2w)]\alpha_\theta$ should be used, that makes the radiation width much smaller, $\gamma_{rad}/\omega_1 \simeq 7 \cdot 10^{-6}$. So, the resonance width is small compared to the frequency gap, and the trapped mode exists.

Let us proceed with impedance estimates. The important quantity entering the stability conditions in circular accelerators, e.g. [2], is so called reduced longitudinal impedance Z/n, where

Z is the total impedance of the ring at given frequency ω, and $n = \omega/\omega_{rev}$ is the corresponding harmonic number of the revolution frequency $\omega_{rev} = c/R$, with R being the machine radius.

If discontinuities are far separated, $g > l_1$, the total impedance of the ring is just a sum of contributions (6) from all $N = 2\pi R/g$ discontinuities. Since $\omega \simeq \omega_1 = \mu_1 c/b$, it leads to the following estimate[2]

$$\frac{Re\, Z}{n} = \frac{NR_1}{n} = \frac{2\pi b}{g\mu_1} R_1 = \frac{8Z_0 A^3}{J_1^2(\mu_1)\delta b^4 g} \,. \tag{40}$$

However, the case of the LHC liner is different, because $g \ll l_1$, and the interaction of discontinuities should be taken into account. One can consider each group of N_{eff} discontinuities as a single combined one, and the number of such group on the ring is $N_g = N/N_{eff} = \pi R/l$. Then the estimate follows from Eq. (40) with replacements $N \to N/N_{eff}$ and $R_1 \to N_{eff}^3 R_1$:

$$\frac{Re\, Z}{n} = N_{eff}^2 \frac{2\pi b}{g\mu_1} R_1 = \frac{16 Z_0 A^2}{\mu_1^2 J_1^2(\mu_1)\delta b g^2} \,, \tag{41}$$

that gives $Re\, Z/n \simeq 424$ Ohms for the narrow-band impedance produced by the trapped modes in the LHC liner, if $RRR = 100$. This value for the narrow-band coupling impedance is too large, even for such a high frequency.

In order to improve and generalize the impedance estimates above, one should consider that the pumping holes are not quite identical, they have some distribution of areas. It results in a frequency spread of resonances produced by different discontinuities. One can take account of the resonance overlapping using a weighted sum in calculating the total impedance of the ring, e.g. [11]:

$$Z_{tot}(\omega) = NZ(\omega) \to N \int dA w(A) Z(\omega, A) \,,$$

where $w(A)$ is the area distribution, $\int dA w(A) = 1$, and $Z(\omega, A)$ is defined by Eq. (5). It is convenient to rewrite $Z(\omega, A)$ at frequencies near the resonance, i.e. when $\omega \simeq \Omega(A) = \omega_1 - \Delta\omega_1(A)$, as follows:

$$Z(\omega, A) \simeq \frac{i\frac{\gamma}{\omega_1} R_1(A)}{1 - \frac{\omega_1}{\omega} + \frac{\Delta\omega_1(A)}{\omega} + i\frac{\gamma}{\omega}} \,,$$

where $R_1(A)$ and $\Delta\omega_1(A)$ are the resonance impedance and frequency shift for the trapped mode caused by a discontinuity with area A. If the resonance width is small enough, namely, $\gamma \ll \Delta\omega_1(A) \ll \omega$, the integral over areas can be treated like a dispersion integral to get

$$Im \int dA \frac{F(A)}{1 - \frac{\omega_1}{\omega} + \frac{\Delta\omega_1(A)}{\omega} + i\frac{\gamma}{\omega}} \simeq -i\pi \frac{F(A_*)}{\left|\frac{d}{dA}\frac{\Delta\omega_1(A_*)}{\omega}\right|} \,,$$

where $A_* = A_*(\omega)$ is the solution to equation $\omega = \omega_1 - \Delta\omega_1(A_*)$.

[2]In the case when γ_{rad} is not small compared to γ_1, in Eqs. (40) and (41) one should replace $2b/\delta$ by ω_1/γ with $\gamma = \gamma_1 + \gamma_{rad}$.

In this way, we obtain two impedance estimates. For far separated discontinuities, i.e. $g \geq l_1$, the frequency shift is given by Eq. (3), and

$$\frac{Re\, Z}{n} \simeq \frac{4\pi Z_0}{\mu_1^2 J_1^2(\mu_1)} \frac{w(A)A^2}{bg}, \tag{42}$$

with A being the averaged area per discontinuity. It should be noted that this estimate is applicable instead of Eq. (40) only when the following *a posteriori* condition

$$\frac{\gamma}{\omega} < \frac{\mu_1^2 A}{\pi b^4 w(A)},$$

is valid. Otherwise, Eq. (42) would give higher value than (40), that is unacceptable because spreading of resonance frequencies due to the area distribution only reduces the impedance.

For interacting discontinuities, $g \ll l_1$, the frequency shift is proportional to the area, cf. Eq. (32), and the impedance estimate is

$$\frac{Re\, Z}{n} \simeq \frac{8\pi Z_0}{\mu_1^2 J_1^2(\mu_1)} \frac{w(A)A^2}{bg}. \tag{43}$$

Surprisingly, it is just twice the result of Eq. (42). For a specific distribution one should take $\max w(A)$ to get maximal impedance estimates (42) and (43). Say, for a Gaussian distribution of areas with standard deviation σ_A, it is $1/(\sqrt{2\pi}\sigma_A)$. If we assume $\sigma_A/A = 0.1$ and apply Eq. (43) for the LHC liner, it gives $Re\, Z/n \simeq 17$ Ohms. This estimate is lower than that from Eq. (41), and it is independent of the wall conductivity and radiation from slots.

It should be noted that an impedance estimate for a liner as a periodic structure, using Eq. (34), would be much higher. However, the periodicity of pumping holes in the liner is violated by the very structure of the accelerator ring, which includes many irregularities like interaction and utility regions, etc. Some intentional additional violation of the hole periodicity is also advisable in order to reduce high-frequency resonances, e.g. [12]. Since even a small distortion of the periodicity drastically reduces the resonance coupling impedance of the structure, see in [12, 13], the estimate (41) is more appropriate for the LHC case.

6 Conclusions

Trapped modes in waveguides with many small discontinuities such as enlargements or holes are studied, both for periodic and non-periodic structures. The existence conditions for trapped modes are considered and their frequencies are calculated. The calculated frequencies are in good agreement with results of numerical computations for particular cases. While our study concentrates on the lowest axisymmetric TM-modes, because of their importance for the beam-chamber coupling impedance calculations, the results can be easily applied for TE- and higher-order modes, using propagation constants for these modes from [1] and formulae of Sections 3-5.

The magnitudes of the narrow-band resonances of the coupling impedance produced by the trapped modes are calculated. These results are applied to obtain coupling impedance estimates for the liners (thermal screens) of large superconducting colliders at frequencies near the cutoff. The practical conclusion for the liner design is to avoid an exact periodicity in the longitudinal distribution of the pumping holes and intentionally introduce some distribution of the hole areas to reduce effects of the trapped modes.

The author would like to express his gratitude to Drs. V.I. Balbekov, R.L. Gluckstern, and G.V. Stupakov for useful discussions.

References

[1] G. Stupakov and S. Kurennoy, *Phys. Rev.* **E49** (1994) 794.

[2] A.W. Chao, *Physics of Collective Beam Instabilities in High Energy Accelerators* (Wiley, New York, 1993).

[3] S. Heifets and S. Kheifets, *Rev. Mod. Phys.* **63** (1991) 631.

[4] S. Kurennoy, *Phys. Part. Nucl.* **24** (1993) 380.

[5] *Design Study of the Large Hadron Collider*, CERN 91-03, Geneva (1991); B. Angerth *et al*, "The LHC beam screen - specification and design", presented at EPAC, London, 1994.

[6] R.E. Collin, *Field Theory of Guided Waves* (IEEE Press, New York, 1991).

[7] K. Halbach and R.F. Holsinger, *Part. Accel.* **7** (1976) 213.

[8] L.A. Vainstein, *Electromagnetic Waves* (Radio i Svyaz', Moscow, 1988).

[9] S. Kurennoy and G. Stupakov, *Part. Accel.* **45** (1994) 95.

[10] S. Kurennoy, Report SSCL-636, Dallas (1993).

[11] V.I. Balbekov, Report IHEP 93-55, Protvino (1993).

[12] S. Kurennoy, *Proceed. of 1993 Part. Accel. Conf.* (IEEE, Washington, 1993) 3417.

[13] V.I. Balbekov, Report IHEP 85-128, Serpukhov (1985).

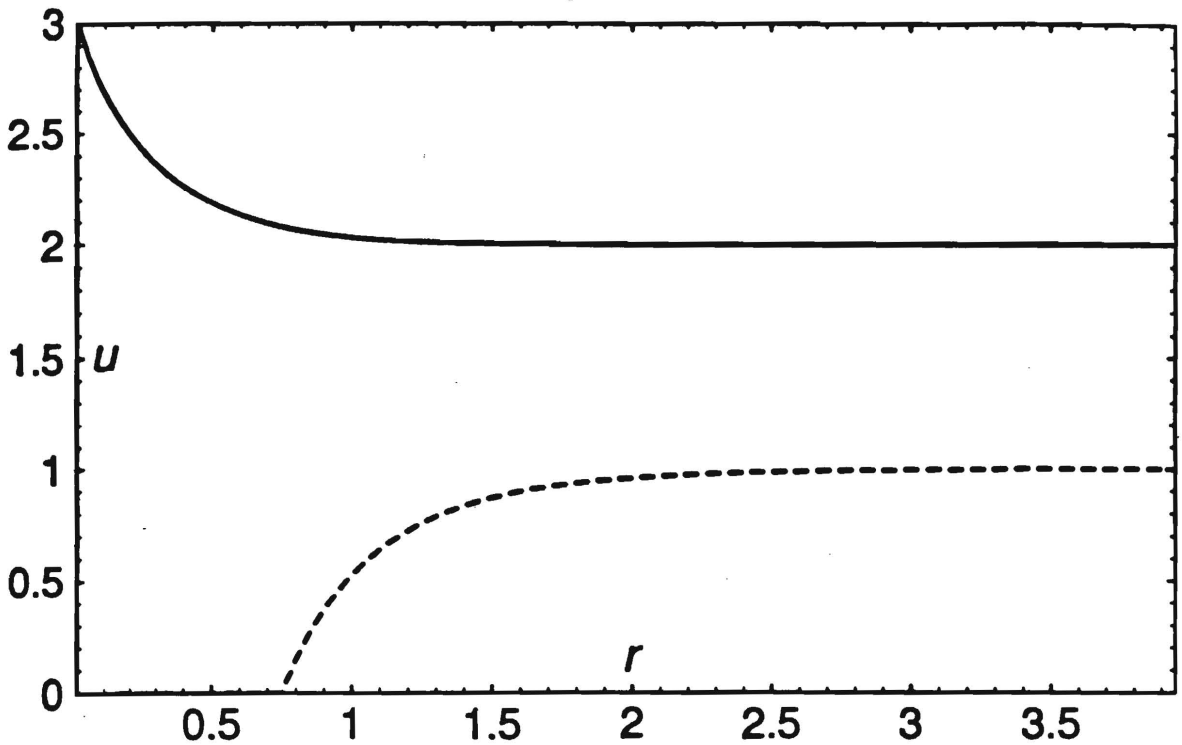

Figure 1: Ratio k/k_1 versus g/l_1 for two discontinuities with $\rho = 2$.

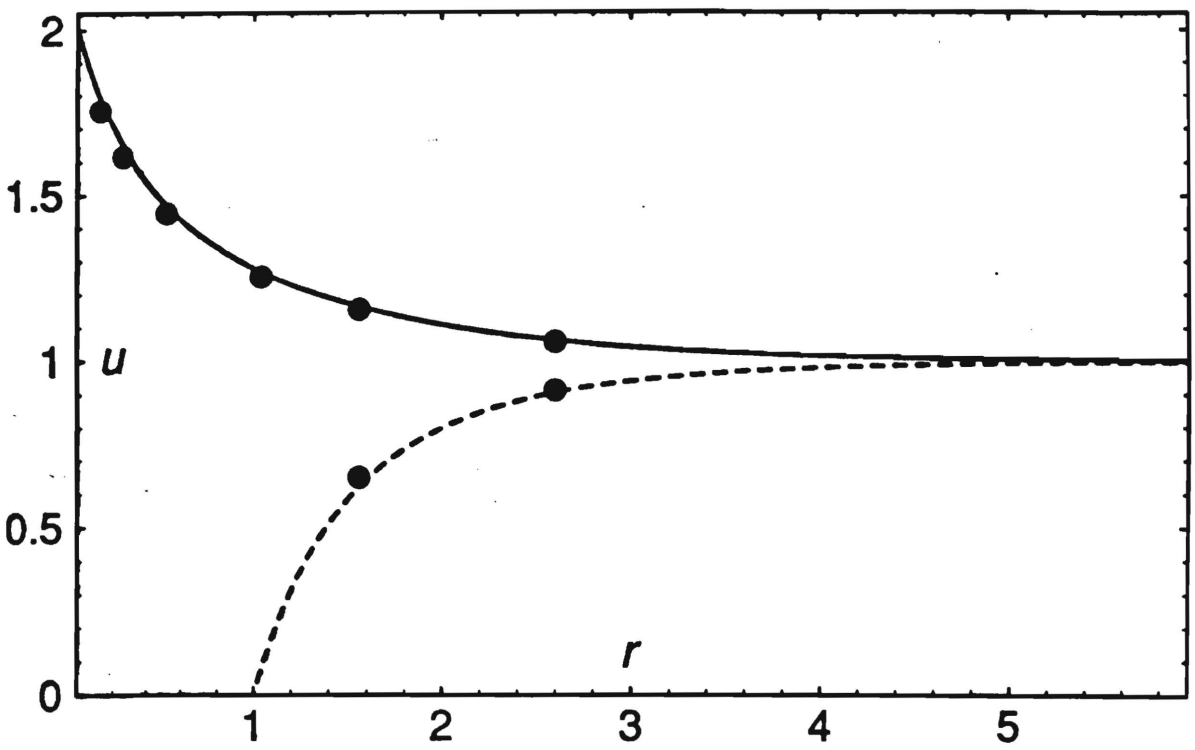

Figure 2: Ratio k/k_1 versus g/l_1 for symmetric (solid line) and antisymmetric (dashed) modes. Thick points show numerical results.

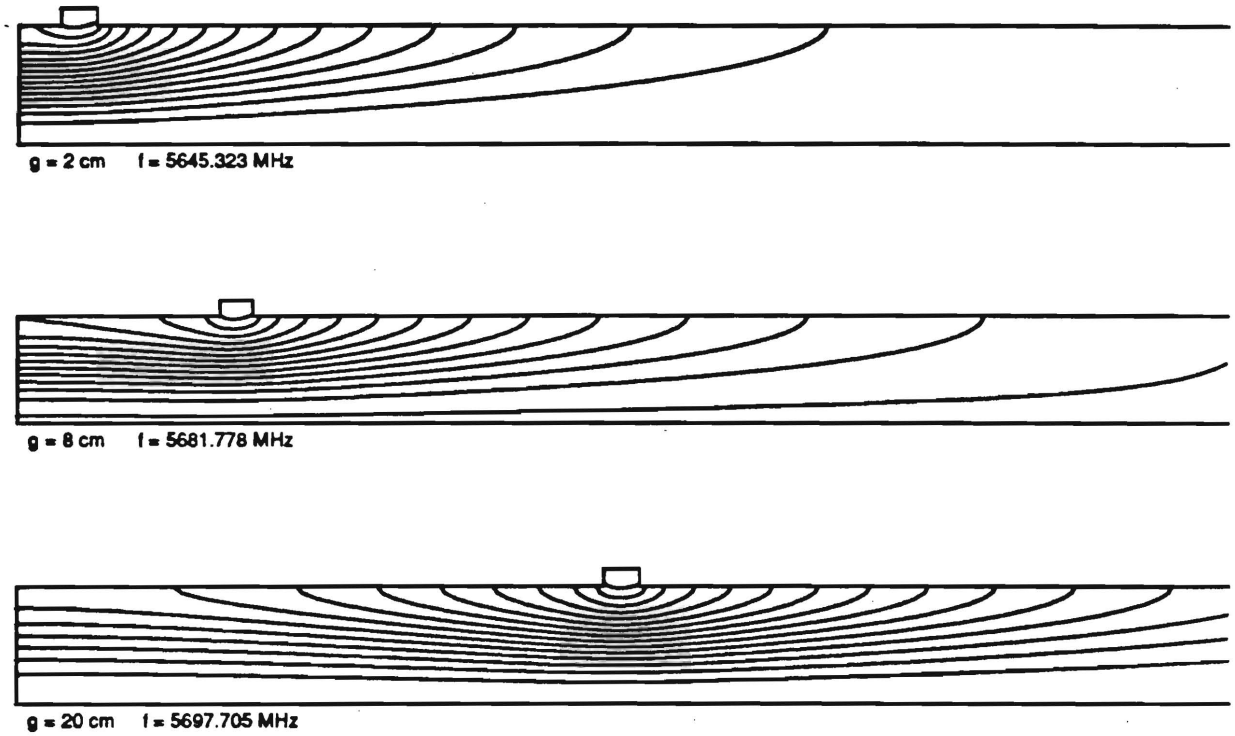

Figure 3: Electric field lines in symmetric trapped modes.

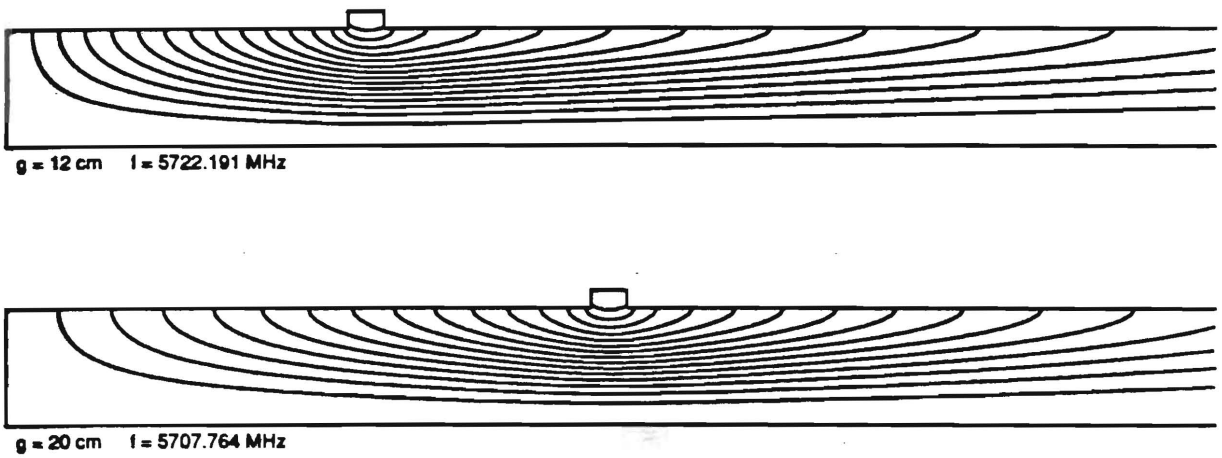

Figure 4: Electric field lines in antisymmetric trapped modes.

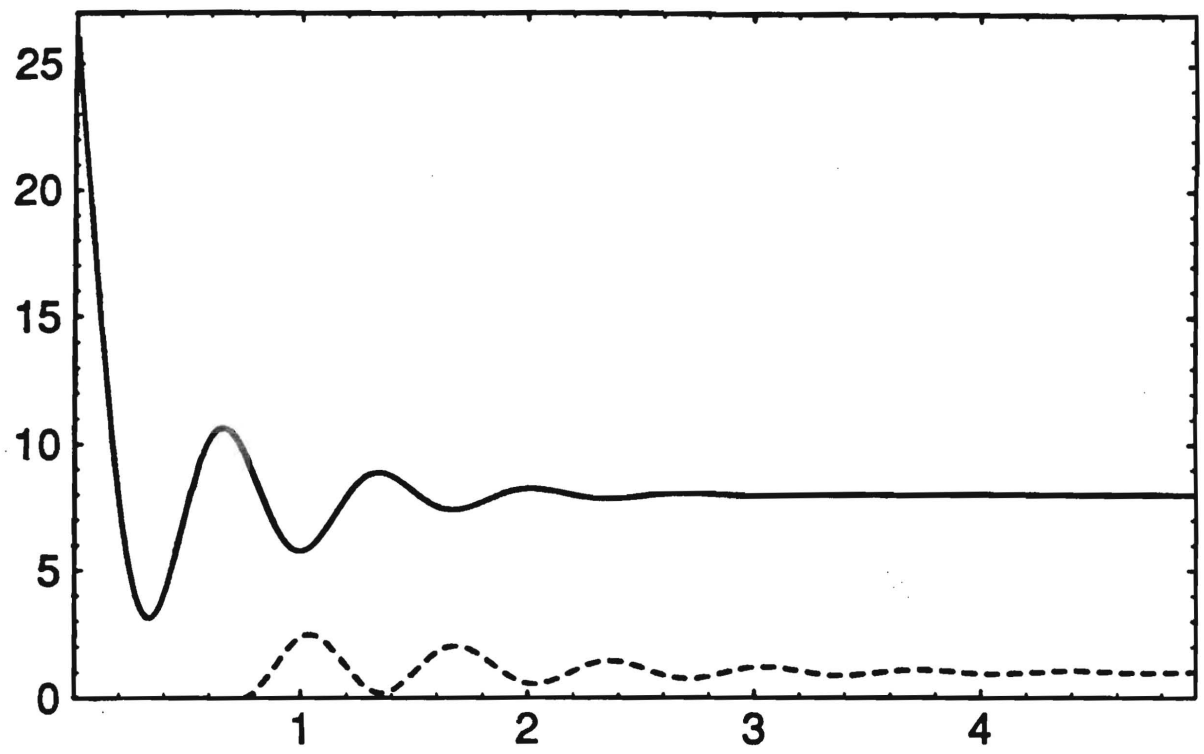

Figure 5: Impedance ratio R_2/R_1 versus g/l_1 for two discontinuities with $\rho = 2$ (parameter $d = 0.26$).

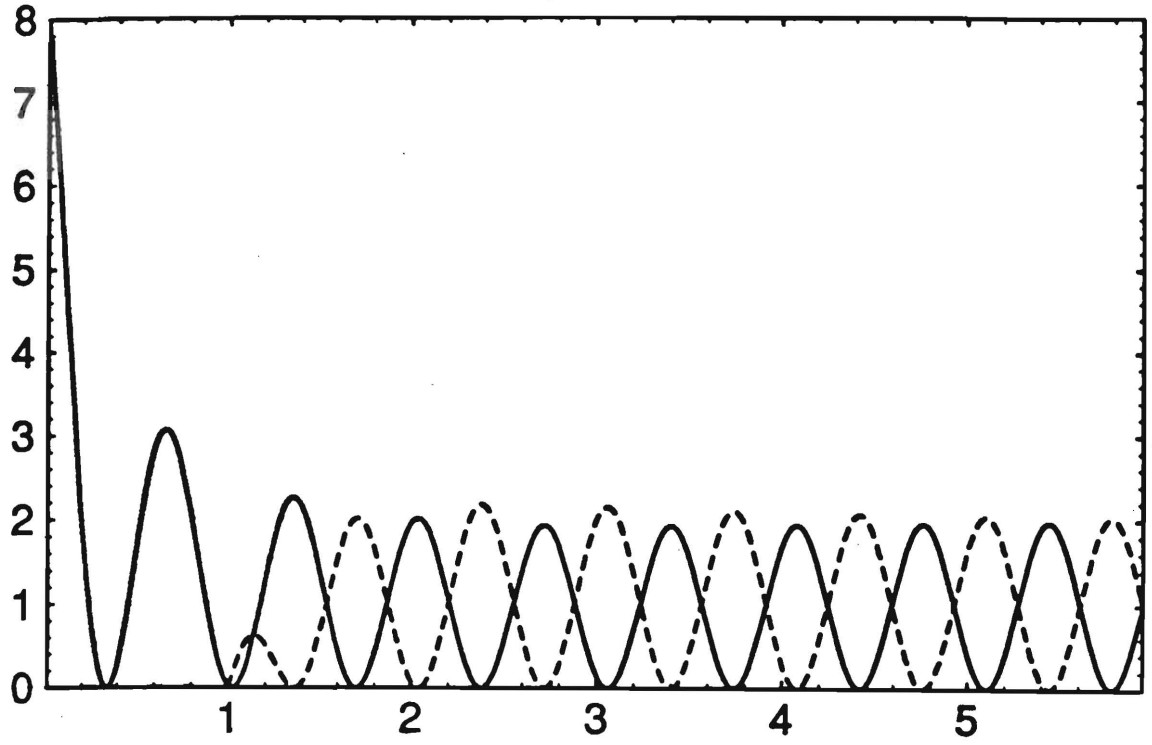

Figure 6: Impedance ratio R_2/R_1 versus g/l_1 for two identical discontinuities ($d = 0.26$). Solid line is for symmetric mode, dashed for antisymmetric one.

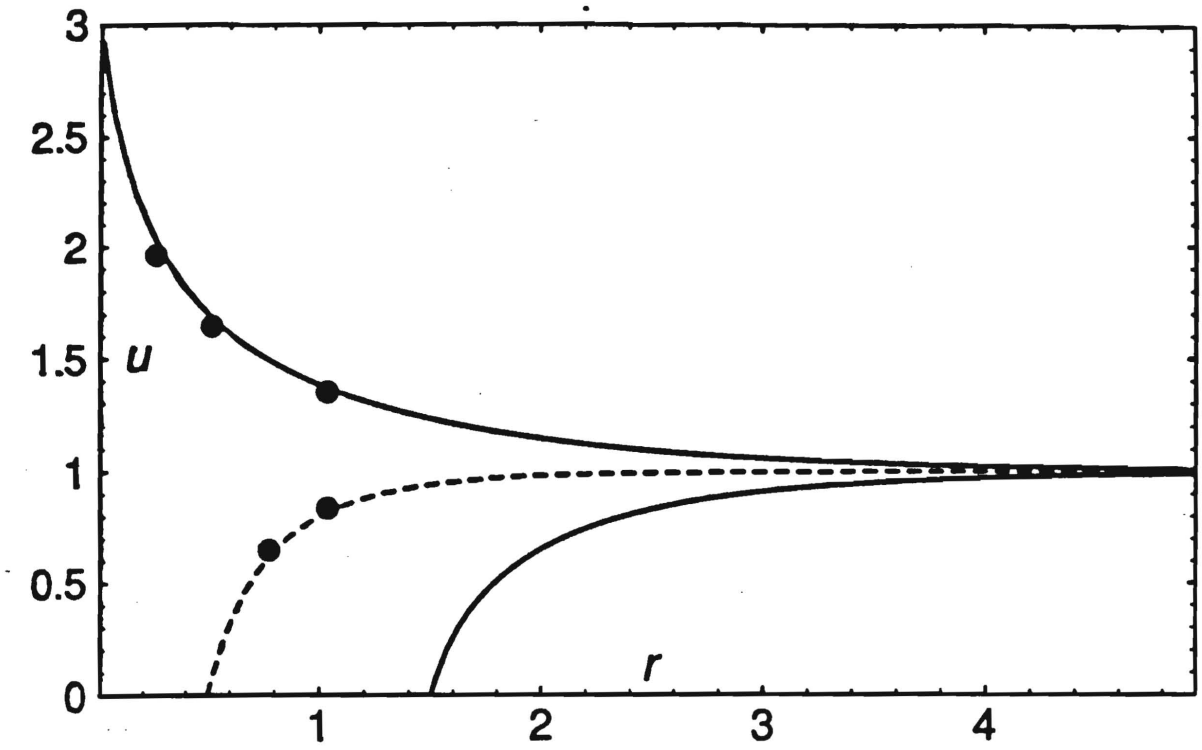

Figure 7: Ratio k/k_1 versus g/l_1 for three identical discontinuities. Solid lines are for symmetric modes, dashed line is for antisymmetric one. Thick points show numerical results.

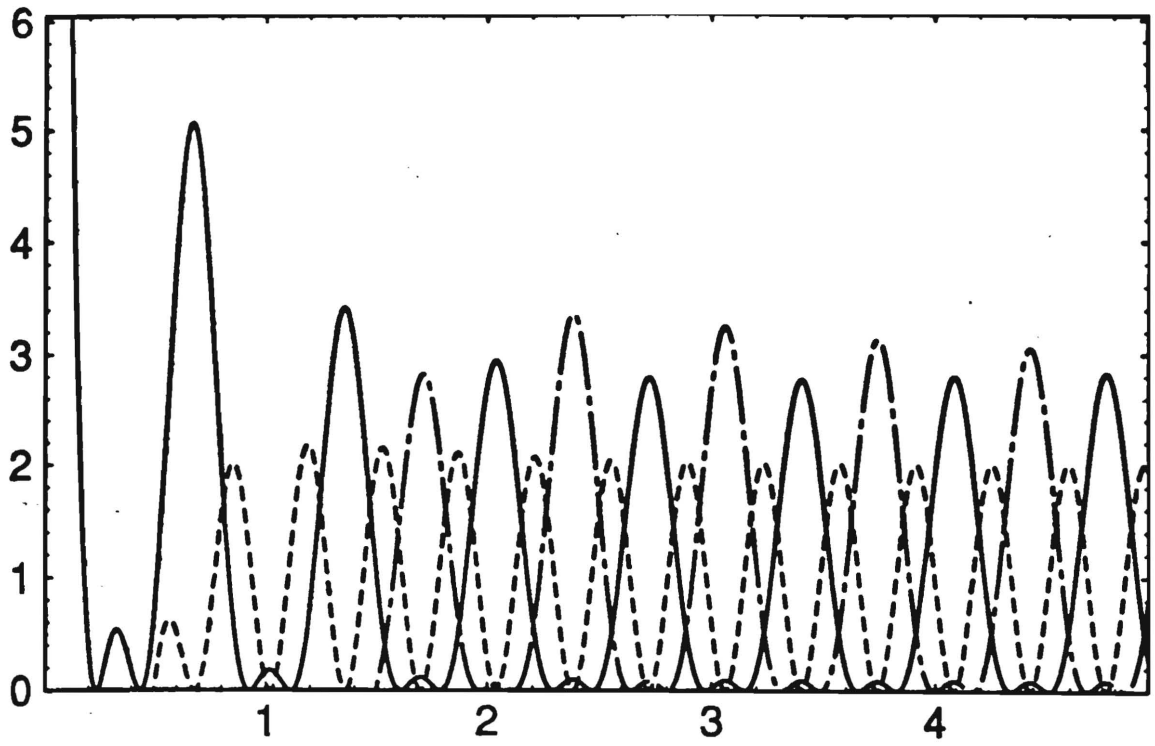

Figure 8: Impedance ratio R_3/R_1 versus g/l_1: solid line for s_0, dashed for a, and dash-dotted for s_1 mode.

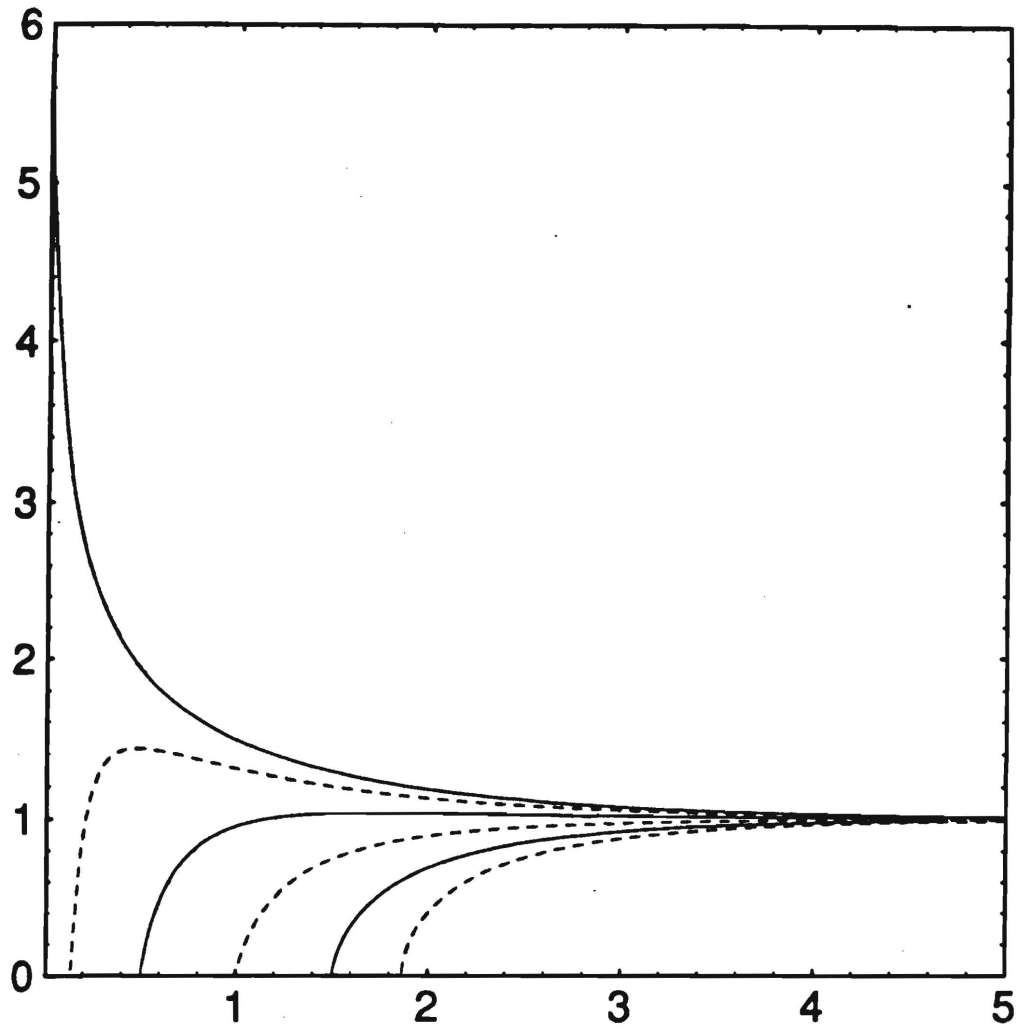

Figure 9: Ratio k/k_1 versus g/l_1 for $N = 6$ identical discontinuities. Solid lines are for symmetric modes, dashed for antisymmetric ones.

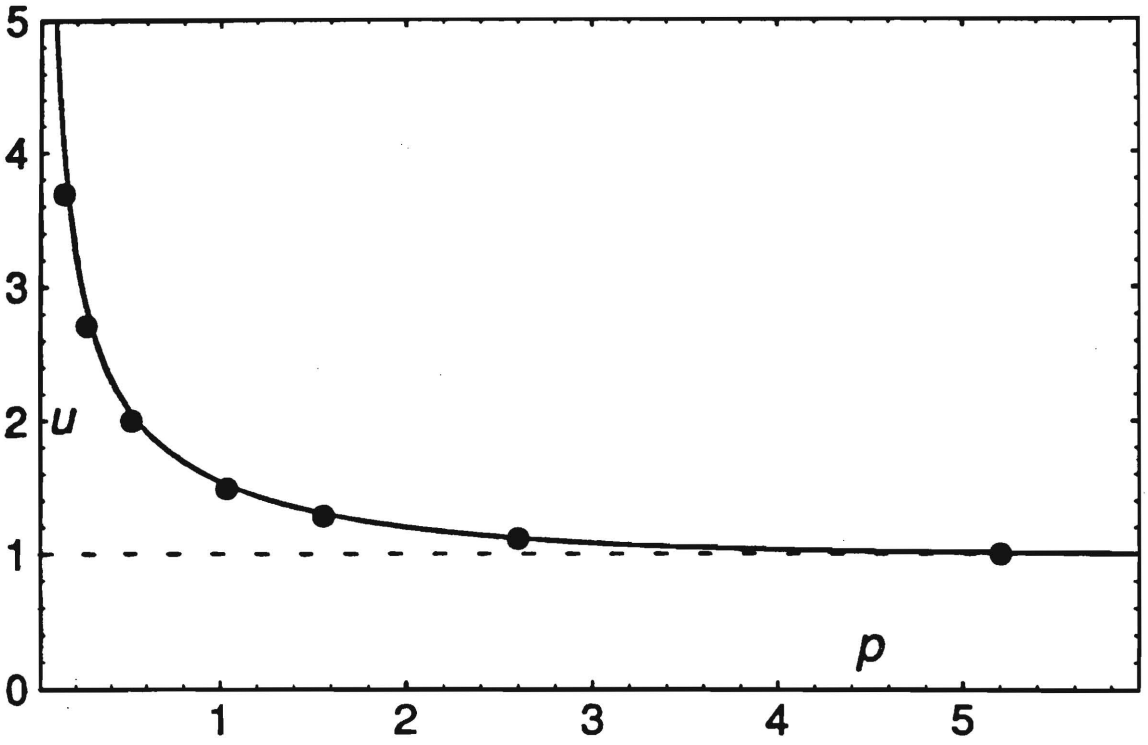

Figure 10: Ratio k/k_1 versus D/l_1 for periodic structures. Thick points show numerical results.

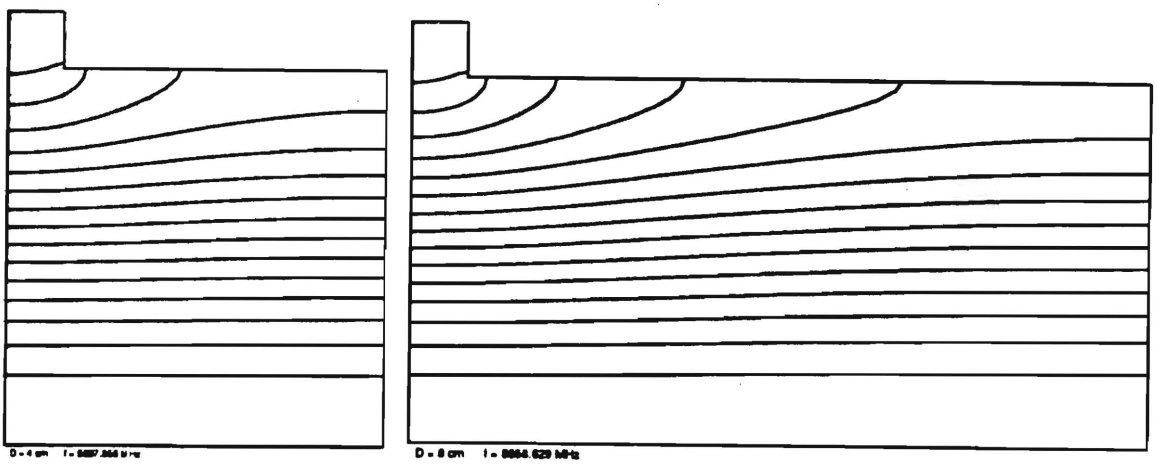

Figure 11: Electric field lines in trapped modes for two periodic structures with different periods.

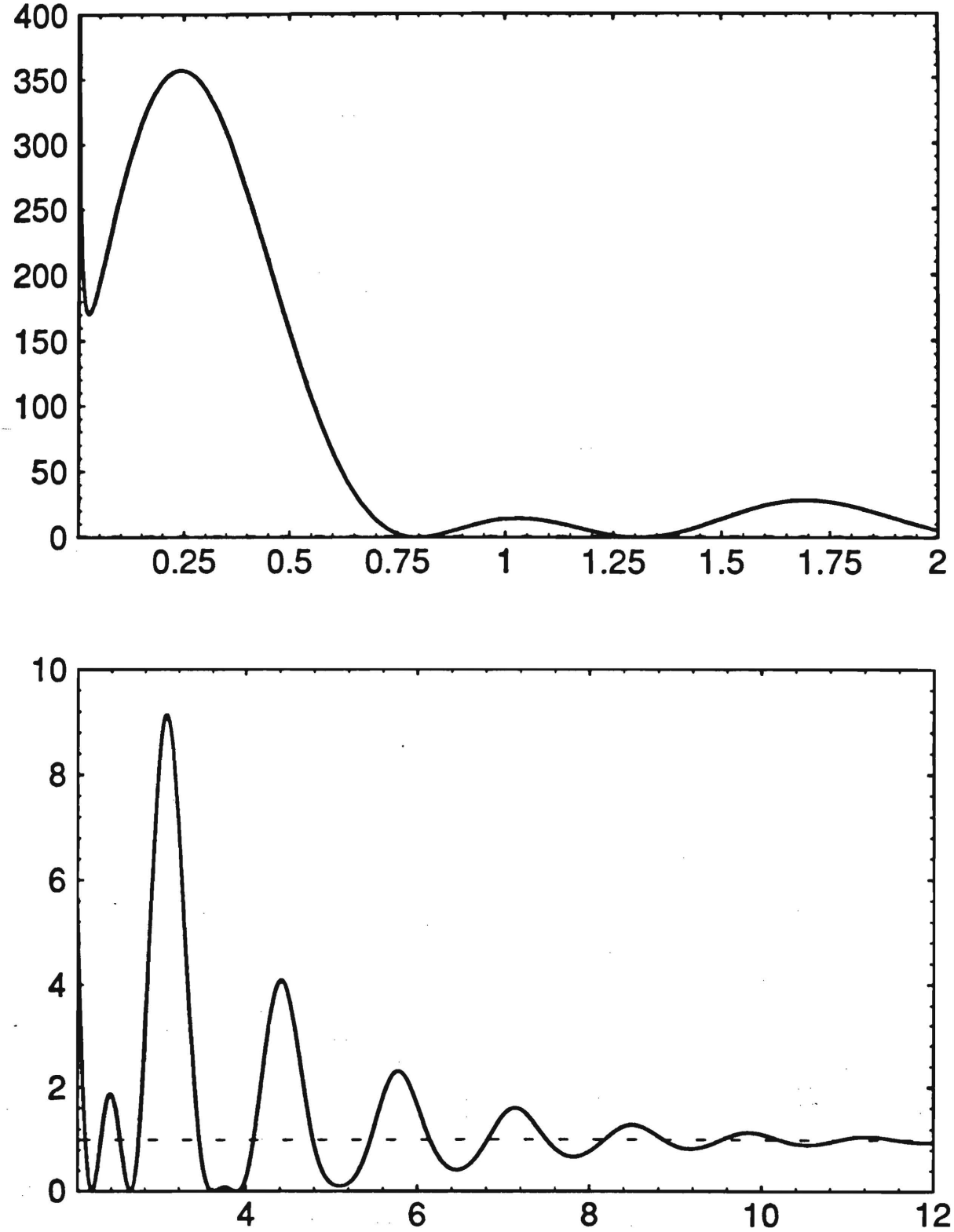

Figure 12: Impedance ratio R_p/R_1 versus D/l_1 for periodic structures with a single discontinuity per period ($d = 0.26$). Two parts of the graph are shown in different scales.

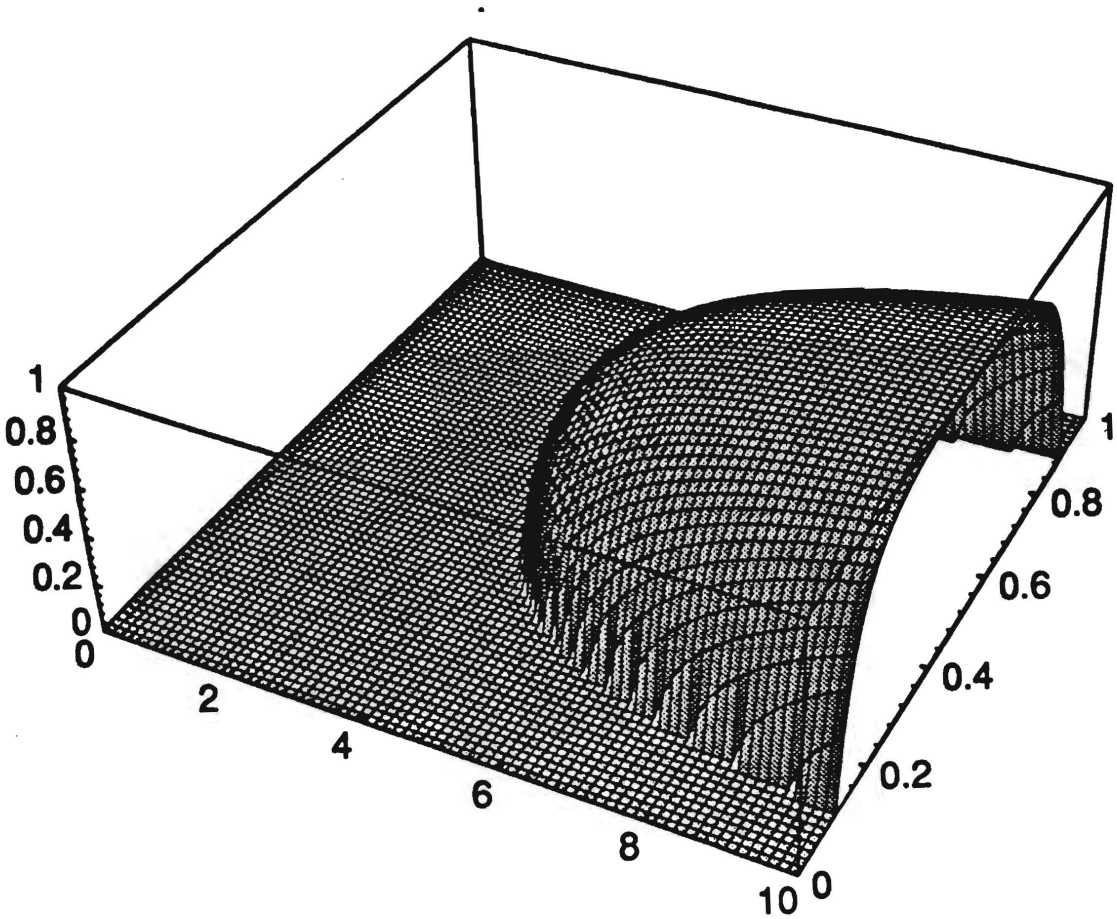

Figure 13: Ratio k/k_1 versus D/l_1 and g/D for periodic structures with two discontinuities per period: antisymmetric mode.

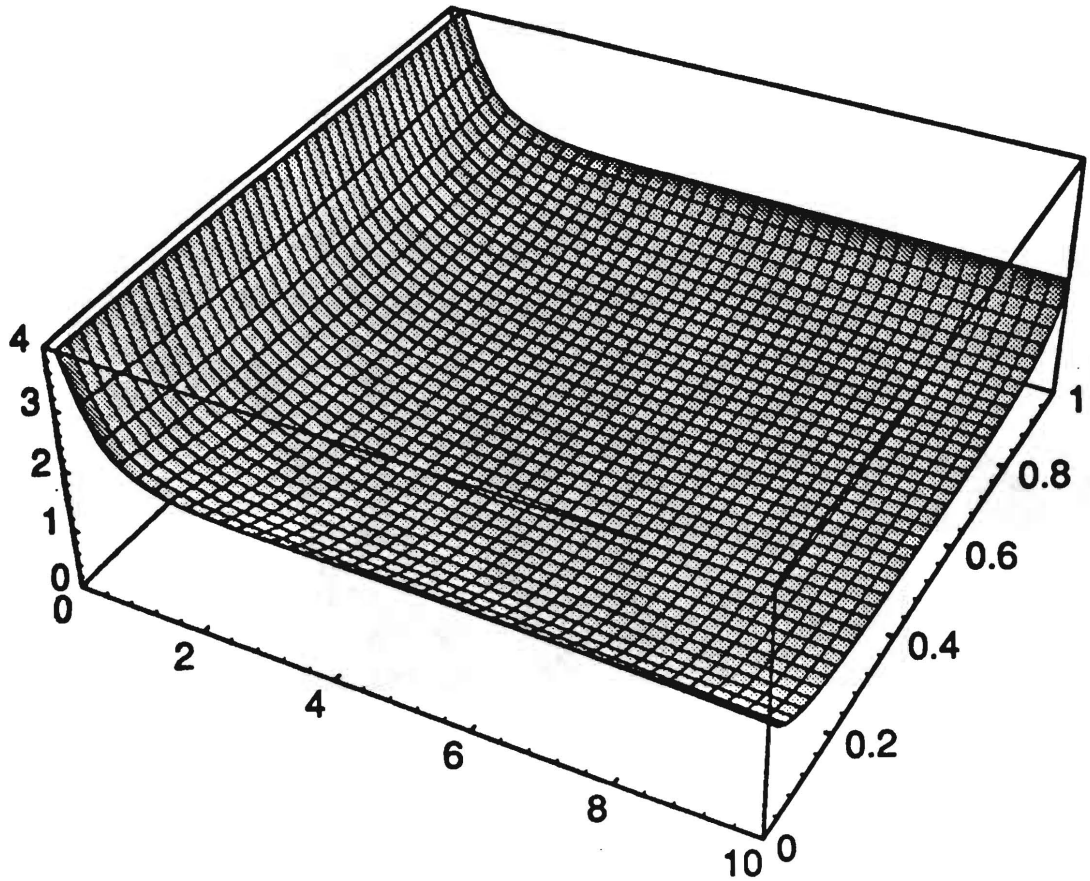

Figure 14: Ratio k/k_1 versus D/l_1 and g/D for periodic structures with two discontinuities per period: symmetric mode.